NLRP6 controls pulmonary inflammation from cigarette smoke in a gut microbiota-dependent manner

Mégane Nascimento, Sarah Huot-Marchand, Manoussa Fanny, Marjolène Straube, Marc Le Bert, Florence Savigny, Lionel Apetoh, Jacques van Snick, Fabrice Trovero, Mathias Chamaillard, et al.

NLRP6 controls pulmonary inflammation to cigarette smoke in a gut microbiota dependent manner

Mégane Nascimento[1], Sarah Huot-Marchand[1], Manoussa Fanny[1], Marjolène Straube[2], Marc Le Bert[1], Florence Savigny[1], Lionel Apetoh[3], Jacques Van Snick[4], Fabrice Trovero[5], Mathias Chamaillard[6], Valérie F.J. Quesniaux[1], Bernhard Ryffel[1], Philippe Gosset[7], Aurélie Gombault[1], Nicolas Riteau[1], Harry Sokol[2,8,9], Isabelle Couillin[1,10*]

[1]*University of Orleans and CNRS, INEM-UMR7355, Orleans, France*

[2]*Sorbonne Université, Inserm, Centre de Recherche Saint-Antoine, CRSA, AP-HP, Hôpital Saint Antoine, Service de Gastroenterologie, F-75012 Paris, France;*

[3]*Indiana University, Indianapolis, United States*

[4]*Ludwig Cancer Research, Brussels, Belgium*

[5]*ArtImmune SAS, 13 avenue Buffon, 45100 Orleans, France*

[6]*Univ. Lille, Inserm, U1003 - PHYCEL - Physiologie Cellulaire, F-59000 Lille, France*

[7]*Institut PASTEUR INSERM U1019, CNRS UMR 8204, Lille, France*

[8]*INRA, UMR1319 Micalis, AgroParisTech, Jouy-en-Josas, France*

[9]*Department of Gastroenterology, Saint Antoine Hospital, Assistance Publique – Hôpitaux de Paris, Sorbonne Universités, Paris, France*

[10]*Lead Contact*

***Address of correspondence to Isabelle Couillin, CNRS, INEM-UMR7355, 3B rue de la Férollerie, 45071 Orleans, France.**

Phone: 0033 238 25 55 02 E-mail: isabelle.couillin@cnrs-orleans.fr

Running Title: NLRP6 in response to lung injury

Grant support by the « Agence nationale de Recherche » **(ANR AAPG2019 CES15 SMOKE6)**, the Centre National de la Recherche Scientifique, the University of Orleans, the Europeen Regional Development Fund (FEDER N° 2016-00110366 and EX005756 and EX016008 TARGET-EX) ExposomeInflam.

Abstract

Chronic obstructive pulmonary disease (COPD) is a major health issue primarily caused by cigarette smoke (CS) and characterized by breathlessness and repeated airway inflammation. NLRP6 is a cytosolic innate receptor controlling intestinal inflammation and orchestrating colonic host-microbial interface. However, its roles in the lungs remain largely unexplored. Using CS exposure models, our data show that airway inflammation is strongly impaired in Nlrp6-deficient mice with drastically less recruited neutrophils, a key cell subset in inflammation and COPD. We found that NLRP6 expression in lung epithelial cells is important to control airway and lung tissue inflammation in an inflammasome-dependent manner. Since gut-derived metabolites regulate NLRP6 inflammasome activation in intestinal epithelial cells, we investigated the link between NLRP6, CS-driven lung inflammation and gut microbiota composition. We report that acute CS exposure alters gut microbiota in both wild type (WT) and Nlrp6-deficient mice and that antibiotic treatment decreases CS-induced lung inflammation. In addition**,** gut microbiota transfer from dysbiotic Nlrp6-deficient to WT mice decreases airway lung inflammation highlighting an NLRP6-dependent gut to lung axis controlling pulmonary inflammation.

Keywords:

NLRP6, Lung inflammation, Cigarette smoke-exposure, Gut microbiota, Gut to lung axis

Graphical abstract

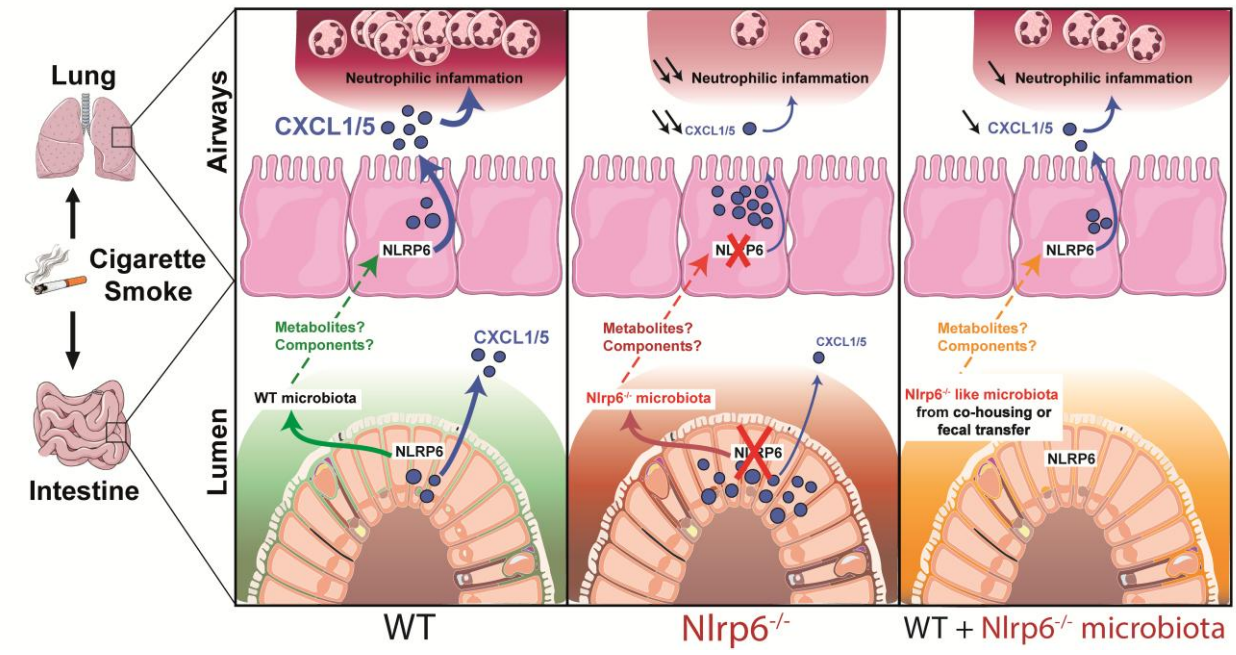

Highlights

- NLRP6 controls lung inflammation to cigarette smoke through CXCL1/CXCL5-mediated neutrophilic influx
- NLRP6-mediated lung inflammation is dependent on the inflammasome
- NLRP6 expression in airway epithelial cells controls lung inflammation to cigarette smoke
- Cigarette smoke exposure alters gut microbiota

- Impaired lung inflammation in cigarette smoke-exposed Nlrp6-deficient mice is transferable to wild type mice by cohousing experiments or fecal microbiota transplantation
- Gut microbiota from Nlrp6-deficient mice limits neutrophilic lung inflammation

Introduction

Chronic obstructive pulmonary disease (COPD) is a severe inflammatory disease characterized by airway obstruction due to bronchial immune cell recruitment and mucus secretion and resulting in impaired lung functions. In a fraction of patients, chronic bronchial inflammation evolve to alveolar disease with alveolar wall destruction, leading to enlargement of airway, that causes shortness of breath and called emphysema [1]. COPD is a major health issue affecting 4 to 10% of the worldwide population and is the third cause of death in the world and 600 million people will suffer from COPD in 2050 if nothing changes [2]. Cigarette smoking is a major societal cause of COPD, counting for more than 95% of cases in industrialized countries [3; 4]. Inflammation can persist even when smoking cessation. Current therapeutics target symptoms, attempting to alleviate chronic inflammation and prevent infection-driven exacerbations however there is no disease-modifying treatment available [5]. Chronic inflammation is characterized by recruitment and activation of innate immune cells in particular neutrophils and macrophages as well as adaptive immune cells such as lymphocytes that produce inflammatory and tissue damaging mediators [6; 7; 8]. Inflammatory neutrophils display increased degranulation and reactive oxygen species release and have been associated with COPD severity [9]. Neutrophils targeting to lung tissue through ELR^+ CXC chemokines (i.e. containing a tripeptide motif glutamic acid-leucine-

arginine and one amino acid between the first two cysteines), essential for both neutrophil influx and activation [10] through signaling on the transmembrane receptors CXCR1 and CXCR2. In particular, CXCL5/LIX (LPS-induced CXC chemokine) is mainly produced by epithelial cells and promote airway neutrophil inflammation [11; 12; 13; 14; 15]. In contrast, alveolar macrophages secrete CXCL1/KC and CXCL2/MIP-2 but not CXCL5/LIX [11]. The important contributions of epithelial cells-derived chemokines to immunity were recently highlighted [16; 17].

Using mouse models of cigarette smoke (CS) exposure and elastase-induced injury, we previously showed that interleukin (IL-) 1β and the adaptor molecule apoptosis-associated speck-like protein containing a CARD (ASC) are essential to promote inflammation, remodeling and emphysema suggesting that inflammasome pathways are involved in the establishment of COPD [18; 19]. Inflammasomes are cytoplasmic multiprotein complexes orchestrating diverse functions during homeostasis and inflammation [20; 21; 22]. These complexes are generally composed of a Nod-like receptor (NLR), ASC adaptor molecule and caspase-1 (Casp-1) or caspase-11 (Casp-11) proteases which activation leads to pro-IL-1β and pro-IL-18 maturation into biologically active IL-1β and IL-18 pro-inflammatory cytokines [20; 21; 22].

NOD-like receptor family pyrin domain containing (NLRP)6 inflammasome composed of NLRP6, ASC and Casp-1 has been shown to regulate microbiota homeostasis and antibacterial immunity in the intestine [23; 24; 25]. NLRP6 inflammasome orchestrates goblet cell mucin granule exocytosis, as mucus accumulation and impaired secretion were observed in Nlrp6-deficient goblet cells [25]. Moreover, recently identified intestinal sentinel goblet cells were shown to non-specifically recognize bacterial compounds leading to NLRP6 inflammasome activation and subsequent calcium-dependent mucin exocytosis from sentinel and adjacent goblet

cells [26]. In addition, NLRP6 expression in inflammatory monocytes reduces susceptibility to chemically-induced intestinal injury [27]. An inflammasome-independent NLRP6 role in the control of enteric virus infection was reported, where NLRP6 interacts with an RNA sensor triggering type I and type III interferon-mediated antiviral responses [28]. In contrast to the gut, NLRP6 role in lung inflammation and repair has been poorly evaluated. A few recent studies showed that this multifaceted innate immune sensor controls neutrophil recruitment and function during pulmonary gram-positive and gram-negative bacterial infections [29; 30; 31].

Here, we demonstrate for the first time that NLRP6 inflammasome governs lung inflammation to CS by controlling neutrophilic inflammation. Impaired lung inflammation in CS-exposed Nlrp6-deficient mice is transferable to WT mice by cohousing experiments or fecal microbiota transplantation. Mechanistically, we show that gut microbiota from Nlrp6-deficient mice regulates lung CXCL5 production and neutrophil influx. Our data also indicate that CS exposure modulates gut microbiota composition in both WT and Nlrp6-deficient mice. In conclusion, we report that smoking induces an unexpected gut to lung axis modulating pulmonary inflammation, which depends on NLRP6 expression in lung and intestinal epithelial cells.

Methods

Mice

Wild type C57BL/6J (WT) mice were purchased from Janvier Labs or bred in our animal facility for microbiota experiments together with gene deficient or conditional mouse strains. $Asc^{-/-}$ mice were given by Francis Derouet at Lausanne University [32], $Casp\text{-}1/11^{-/-}$ by Seshadri Tara at BASF Bioresearch corporation [33] and $Nlrp6^{-/-}$ by Mathias Chamaillard at Lille Pasteur Institute [24]. Nlrp6 flox/flox mice are from Philip Rosenstiel Institute of clinical Molecular Biology,

Kiel, Germany. Nlrp6 tissue specific knockouts were obtained by breeding Nlrp6 flox/flox with Aqp5Cre knock-in (Acid or Aqp5tm1.1(cre,DsRed)Pfl), allowing deletion in alveolar type I (AT1) cells in adult lung [34]. All mouse strains were backcrossed 10 times or made on C57Bl/6J background and housed at the animal facility at Transgenose Institute (UPS-TAAM) in CNRS Orleans, France. Except for cohousing experiments, 6-10 weeks old mice were kept in sterile, isolated and ventilated cages. All animal experiments followed the French government's ethical and animal experiment regulations (CLE CCO 2015-1088).

Cigarette smoke exposition

3R4F cigarettes (University of Kentucky) were used without filter. Mice were placed in an InExpose smoke chamber (EMKA Technologies) and inhaled smoke from 4 cigarettes, 3 times a day for 4 days for acute inflammation model or 4 cigarettes, 3 times a day, 5 days a week for 6 weeks for subchronic inflammation model. Bronchoalveolar lavage (BAL) and lung tissue were collected about 16 hours after the last CS exposure.

Broncho-alveolar lavage (BAL)

BAL was performed as previously described [19]. Differential cell counts were performed by counting an average of 250 cells on Cytospin preparations (Shandon CytoSpin 3, ThermoFisher Scientific) after May-Grünwald-Giemsa staining (RAL-Diff Quick, Siemens) according to manufacturer's instructions.

Tissue homogenates

Lungs were perfused with Isoton (Beckman Coulter) to flush the vascular content. Washed lungs and ileum were homogenized by a rotor-stator (Ultra-turrax) in PBS with protease inhibitor cocktail (Roche) for mediator measurement or in RIPA buffer with protease inhibitor cocktail

(ThermoFisher Scientific) for immunoblotting analysis. Extracts were centrifuged and supernatants stored at -80°C.

Lung histology

Lung left lobe was fixed in 4% buffered formaldehyde (MMFrance), processed and paraffin embedded under standard conditions. 3µm lung sections were stained with Direct Red 80 (Red Sirius, Sigma-Aldrich). The slides were blindly examined at 10X magnification (Leica) and cell infiltration assessed by a semi-quantitative score (with increasing severity 0-5) by two independent investigators.

Mediator measurements

BALF supernatants and lung homogenates mediators were measured by ELISA assay kits for murine MPO, IL-1β, CXCL1, CXCL5, CXCL15, BAFF, LCN2, MMP-9 and TIMP-1 (R&D System) according to manufacturer's instructions.

Air Liquide Interface (ALI) Trachea epithelial cells culture

Mice trachea were collected from Wild type C57BL/6J (WT). Using pronase (1,5mg/mL) (Roche®), tracheas were digested over night at 4°C. Digestion was stopped using MTEC/Basic medium (Composition Table X) + 10% fetal bovine serum (FBS). DNAase (0,5mg/mL) (Sigma-Aldrich®) step was realized in MTEC/Basic medium without FBS. Adherent cells were removed by plating samples on specific petri dish (Primaria Corning). 33.10^3 of trachea epithelial cells were plated in 150 µL of MTEC/Plus medium (Composition Table X) on rat-tail collagen (0,05mg/mL diluted in acetic acid 20mM) (Thermofisher®) pre-coated transwells. Then, MTEC/Plus medium was added in down transwell part. Trachea epithelial cell grown 4 days at 37°C in 5% of CO2.

At day 4, medium was changed with MTEC/Plus medium until cell confluence. Then, trachea epithelial cells up medium was removed and cells were washed with Phosphate Buffered Saline (PBS). Down medium was changed every day during 1 week with MTEC/SF differentiation medium (Composition Table 1). Trachea epithelial cell in ALI grown at 37°C in 5% of CO2 until cell collection or stimulation.

MTEC/Basic	**Concentration**
Hepes	15,000 mM
Pen/strep	1 X
MTEC/Plus	**Concentration**
Insulin Transferrin cocktail 1X (Thermofisher®)	10 µg/mL
Cholera toxin (Sigma Aldrich®)	0,1 µg/mL
Epidermal Growth Factor (EGF) (Sigma Aldrich®)	0,025 µg/mL
Bovin Pituitary Extract (Fisher Gibco®)	30 µg/mL
FBS	5%
Retinoic Acid B (RA-B) (Sgma Aldrich®)	0,05 µM
MTEC/NS	**Concentration**
NuSerum	2%
Retinoic Acid B (RA-B) (Sgma Aldrich®)	0,05µM
MTEC/SF	**Concentration**
Insulin Transferrin cocktail 1X (Thermofisher®)	5 µg/mL
Cholera toxin (Sigma Aldrich®)	0,025 µg/mL
Epidermal Growth Factor (EGF) (Sigma Aldrich®)	5ng/mL
Bovin Pituitary Extract (Fisher Gibco®)	30µg/mL
Commercial BSA solution (steril) (Sigma Aldrich®)	1mg/mL
Retinoic Acid B (RA-B) (Sgma Aldrich®)	0,05µM

Table 1: *Trachea epithelial cells culture medium compositions*

Specific *Nlrp6* RT-PCR on trachea epithelial cells

Total RNA was extracted from epithelial cells using isolation kit (RNeasy kit®) following the manufacturer's protocol. RNA concentration and integrity were determined using a Nanodrop (Nd-1000) spectrophotometer (Labtech®). Reverse transcription of RNA into cDNA was carried out with GoScript™ Reverse Transcription System (Promega®). Using iScript RT supermix (BioRad®) 500ng of total RNA was subjected to Reverse Transcription. PCR was performed on 8.75µg of synthetized cDNA. Specific primers used for *Nlrp6* mRNA amplification were as follows: *Nlrp6* forward 5'-GAC-CAG-TTT-AGC-CCA-GAA-AAG-G-3'; *Nlrp6* reverse 5'-CTC-CAG-TGT-AGC-CAT-AAG-CAG- 3'. PCR program is described in table 2.

Initialisation	94°C, 2min			
	5 Cycles	5 Cycles	5 Cycles	5 Cycles
Denaturation	94°C, 30s	94°C, 30s	94°C, 30s	94°C, 30s
Annealing	62°C, 30s	61°C, 30s	59°C, 30s	58°C, 30s
Elongation	72°C, 1min	72°C, 1min	72°C, 1min	72°C, 1min

Table 2: *PCR used program.*

FLAG Immunohistochemistry

Lungs were fixed with 4% paraformaldehyde (Sigma-Aldrich®) for 72h, embedded in paraffin and sectioned at 3 µm. Lung sections were dewaxed and rehydrated, then heated 20 min at 80°C in citrate buffer 10 mM pH=6 for antigen retrieval (unmasking step). Lung sections were permeabilized in PBS 0.5% triton X-100, blocked with 5% FCS for 1h at RT and then incubated overnight with primary mouse anti-FLAG (1:100, A9542 Sigma). After washing, sections were incubated with with the appropriate second antibody conjugated to horseradish peroxidase (1:200 anti-mouse IgG, Sigma Aldrich®) in 1% FCS 1h at RT. Following washing, lung sections were incubated with HRP Substrate, DAB (Vector Laboratories®), following the manufacturer's protocol. After distilled water washing, Gill hematoxyline counterstaining on lung sections was

done. Then, lung sections were dehydrated, fixed and mounted onto microscope slides (Eukitt). Slides were examined by using a scanner NDP view.

Treatments

Mice were anesthetized by intra-muscular injection of ketamine (10mg/mL, Merial) and xylasine (0.2%, Bayer). Recombinant murine CXCL5/LIX (9-78 amino acid, 1µg per mouse) was administered intranasally at day 2 and 4 between the second and the third daily exposition. Anti-CXCL5/LIX antibody was obtained from Jacques Van Snick. 150µg per mouse was injected intraperitoneally at day 2 and 4 between the second and the third daily expositions. Antibiotic cocktail containing Vancomycin 0.5g/L (Sandoz), Ampicillin 1g/L (Euromedex), Neomycin 1g/L (Euromedex), Metronidazole 1g/L and sucrose 1% (Sigma-Aldrich) diluted in sterile water was given in drinking water and replaced every 3 days.

Generation of bone marrow chimeras

CD45.1 WT and CD45.2 Nlrp6$^{-/-}$ recipient mice were lethally irradiated [35] and 4x10^{6} NLRP6-deficient or WT bone marrow cells were injected into the lateral tail vein 24h after. Four chimeric mouse groups were obtained: WT>WT, NLRP6$^{-/-}$>WT, WT>NLRP6$^{-/-}$, NLRP6$^{-/-}$ >NLRP6$^{-/-}$. Bone marrow reconstitution was controlled by flow cytometry assessing the ratio of CD45.1 versus CD45.2 blood immune cells. Three months after bone marrow reconstitution, mice were exposed to air or CS as described.

Cohousing experiments

Immediately after weaning, WT and Nlrp6$^{-/-}$ gender-matched animals were co-housed at 1:1 ratio for 12 weeks and mice were exposed to air or CS as described.

Fecal transplantation

Fecal transplantation was performed as previously described [35]. Briefly, 3-week old germ-free C57BL6/J (WT) mice generated in-house in sterile isolators (TAAM-CNRS) were orally transplanted with 200µl fecal homogenates from SPF-WT or SPF-Nlrp6$^{-/-}$ mice. Mice were maintained in isolator until 7 weeks of age, placed in conventional breeding facility for one week for adaptation and exposed to CS for 4 days.

Quantitative RT-PCR

Total RNA was isolated from homogenized mouse lung using Tri Reagent (Sigma-Aldrich) and quantified by NanoDrop (Nd-1000). Reverse transcription of RNA into cDNA was carried out with GoScript™ Reverse Transcription System (Promega). RT-qPCR was performed with Fast GoTaq qPCR Master Mix (Promega) on ARIA MX (Agilent Technologies). *Mmp12* primers were purchased from Qiagen. RNA expression was normalized to *Gapdh* (Qiagen) expression and analysed using the $^{\Delta\Delta}$Ct method.

Immunoblotting

Protein concentrations in tissue homogenates were determined using Pierce BCA protein assay (ThermoFisher Scientific). 40 µg of proteins were denatured by boiling (95°C, 5 min) in reducing SDS sample buffer, separated by SDS-PAGE and transferred to nitrocellulose membranes (GE Healthcare). Membranes were blocked 2 hours in 5% Blotting-Grade Blocker (BioRad), washed three times in Tris-Buffered saline (TBS)- 0,1% Tween 20 and incubated with primary rabbit anti-murine LIX antiboby (Peprotech) overnight at 4°C. Membranes were washed three times in TBS- 0,1% Tween 20 and incubated with the appropriate secondary antibody conjugated to

horseradish peroxidase (HRP) 1 hour at room temperature (RT). Membranes were incubated with mouse anti-actin HRP-conjugate (Sigma-Aldrich) in 5% Blotting-Grade Blocker in TBS-0,1% Tween 20 for 1 hour at RT. Detection was performed with ECL Prime Western-blotting Detection Reagent (GE Healthcare) and Multi-application gel imaging system PXi software (Syngene).

Immunostaining

Lungs and ileum were fixed in 4% paraformaldehyde (PFA) (Sigma-Aldrich) and then dehydrated in 30% sucrose (Sigma-Aldrich) solution for 2 weeks. Organs were embedded in Tissue-Tek® OCT™ (Sakura) and store at -80°C prior to be sliced. Sections were incubated for 30 minutes in pre-heated antigen retrieval buffer (Citrate buffer 10mM pH=6). Sections were incubated in TBS-Triton X-100 0.1% and then in blocking solution containing 1% bovine serum albumin (BSA) -10% fetal bovine serum (FBS) -0.1% Triton X-100 in TBS. Primary antibody directed against CXCL5 (Peprotech) was incubated in blocking solution over night at 4°C. Sections were rinsed three times in TBS and incubated with appropriated secondary antibody. Slides were counterstain using 4′,6-diamidino-2-phenylindole (DAPI) for 10 minutes, rinsed and coverslip were mount with Fluoromount-G medium (SouthernBiotech). Images were treated using ImageJ software.

Stool collection and DNA extraction

Feces were collected and immediately frozen at -80°C for further analysis. DNA was extracted from the fecal samples as described [36]. Following microbial lysis by both mechanical and chemical methods, nucleic acids were precipitated in isopropanol for 10 minutes at room temperature, incubated for 15 minutes on ice and centrifuged for 30 minutes at 20,000 g at 4°C.

Pellets were resuspended in 450 μL of phosphate buffer and 50 μL of potassium acetate. After RNase treatment and DNA precipitation, nucleic acids were recovered via centrifugation at 20,000 g at 4°C for 30 minutes. The DNA pellet was resuspended in trypsin-EDTA buffer. DNA samples were then subjected to 16S sequencing.

16S rRNA sequencing

Bacterial diversity in stools was determined by targeting a portion of the ribosomal genes in extracted DNA. A 16S rRNA gene fragment comprising the V3 and V4 hypervariable regions (16S sense 5′-TACGGRAGGCAGCAG-3′ and antisense 5′-CTACCNGGGTATCTAAT-3′) was amplified using an optimized and standardized 16S-amplicon-library preparation protocol (Metabiote, GenoScreen, Lille, France). Briefly, 16S DNA PCR was performed using 5 ng of genomic DNA according to the manufacturer's protocol (Metabiote), 192 bar-coded primers (Metabiote MiSeq Primers) at final concentrations of 0.2 μmol/L and an annealing temperature of 50°C for 30 cycles. The PCR products were purified using an Agencourt AMPure XP-PCR purification system (Beckman Coulter, Brea, CA, USA), quantified according to the manufacturer's protocol, and multiplexed at equal concentrations. Sequencing was performed using a 300-bp paired-end sequencing protocol on an Illumina MiSeq platform (Illumina, San Diego, CA, USA) at GenoScreen, Lille, France. Raw paired-end reads were subjected to the following processes: (1) quality-filtering using the PRINSEQ-lite PERL script (Schmieder R, Edwards R. Quality control and preprocessing of metagenomic datasets. Bioinformatics 2011;27:863-4), by truncating the bases from the 3′ end, that did not exhibit a quality <30, based on the Phred algorithm; (2) paired-end read assembly using fast length adjustment of short reads to improve genome assemblies (FLASH) (Magoc T, Salzberg SL. FLASH: fast length adjustment

of short reads to improve genome assemblies. Bioinformatics 2011;27:2957-63.) with a minimum overlap of 30 bases and a 97% overlap identity; and (3) searching for and removing both forward and reverse primer sequences using CutAdapt, with no mismatches allowed in the primer sequences. Assembled sequences, for which perfect forward and reverse primers were not found, were eliminated.

16S rRNA sequence analyses

The sequences were demultiplexed and quality filtered using the QIIME version 1.9.1 software package [37]. The sequences were then assigned to operational taxonomic units (OTUs) using the UCLUST algorithm with a 97% pairwise identity threshold and classified taxonomically using the Greengenes reference database (version 13.5). Rarefaction was performed (32,000 sequences per sample) and used to compare the relative abundance of OTUs across samples. Beta diversity was measured by a Bray Curtis distance matrix and was used to build principal coordinate analysis (PCoA) plots. Raw sequence data are accessible in the European Nucleotide Archive.

Statistical analysis.

Statistical evaluation of differences between experimental groups was determined by one-way ANOVA, analysis of variance, Bonferroni test for *in vivo* experiments and one-way ANOVA using Prism software (La Jolla, CA, USA). *P* values <0.05 were considered statistically significant. All tests were performed with Graphpad Prism, Version 8 for Windows (GraphPad Software Inc.). Data are expressed as mean ± SEM. Statistically significant differences were defined as follow: *P<0.05, **P<0.01, ***P<0.001 and****P<0.0001).

Results

Nlrp6 deficiency dampens lung inflammation and remodeling to CS exposure

Since NLRP6 was shown to regulate intestinal epithelium homeostasis and immunity [24; 25; 28], we asked whether it could control pulmonary epithelium function and airway inflammation following cigarette smoke (CS) exposure. Wild type (WT) and Nlrp6-deficient ($Nlrp6^{-/-}$) mice were subchronically exposed to CS three times a day, five days a week for six weeks. As compared to unexposed (Air) mice, subchronically-exposed WT mice (CS) display elevated numbers of bronchoalveolar fluid (BALF) cells (Fig. 1A), mainly macrophages (Fig. 1B), neutrophils (Fig. 1C) and lymphocytes (Fig. 1D), which were all strongly attenuated in CS-exposed $Nlrp6^{-/-}$ mice. Among immune cells, neutrophils play a major role in response to CS [38; 39]. As a marker of neutrophil recruitment, myeloperoxidase (MPO) was significantly reduced in the BALF and the lungs (Fig. 1E and F) of CS-exposed $Nlrp6^{-/-}$ mice. In comparison, neutrophilic chemokine CXCL1 production was significantly decreased in the BALF of $Nlrp6^{-/-}$ mice (Fig. 1G) but not in lung homogenates (Fig. 1H). Since NLRP6 was shown to regulate IL-1β and IL-18 production through inflammasome activation, we analyzed IL-1β lung expression and show that its CS-mediated induction was significantly attenuated in $Nlrp6^{-/-}$ mice (Fig. 1I). In addition, as a correlate of B lymphocyte recruitment and disease severity [40], B cell activating factor (BAFF) induction following CS-exposure was significantly reduced in the BALF of $Nlrp6^{-/-}$ as compared to WT mice (Fig.1J).

We next measured proteases involved in COPD establishment and in particular matrix metalloproteinase (MMP) and their inhibitors (TIMP). MMP-9 protein levels in BALF and lungs (Fig. 1K and L), *Mmp-12* mRNA expression in lungs (Fig. 1M) and tissue inhibitor of MMP (TIMP)-1 protein levels in BALF and lungs (Fig. 1N and O) were significantly decreased in

subchronically CS-exposed Nlrp6$^{-/-}$ mice as compared to WT mice. Lung microsections and histology analysis showed reduced inflammation in Nlrp6$^{-/-}$ mice in comparison to WT mice (Fig. 1P). In addition, acute CS exposure during 4 days confirmed reduced inflammation in Nlrp6$^{-/-}$ in comparison to WT mice. While total BAL cells numbers were not significantly changed (Fig. S1A), we report a strong reduction of neutrophils (Fig. S1B), MPO levels (Fig. S1C) in the BAL, IL-1β levels (Fig. S1D) but not IL-18 (Fig. S1E) in the lungs. BALF levels of CXCL1/KC were significantly reduced in Nlrp6$^{-/-}$ mice (Fig. S1F) but not in lung homogenates (Fig. S1G) as observed upon subchronical exposure. We also observed reduced MMP-9 levels in BALF and lungs (Fig. S1, H and I), *Mmp-12* mRNA expression in lungs (Fig. S1J) and TIMP-1 protein levels in BALF and lungs (Fig. S1, K and L) in Nlrp6$^{-/-}$ mice as compared to WT mice. Lung microsections and histology analysis showed reduced inflammation in Nlrp6$^{-/-}$ mice in comparison to WT mice (Fig. S1M).

In addition, to verify that mouse genetic background and/or housing were not responsible for the difference in inflammatory response to CS observed, we performed breeding between Nlrp6$^{+/-}$ mice in order to obtain Nlrp6$^{+/+}$ and Nlrp6$^{-/-}$ littermates (Fig. S2A) and we acutely exposed them to CS exposure. Importantly we confirmed that neutrophil number and percentage in BALF (Fig. S2B-C), MPO levels (Fig. S2D-E), IL-1β in lungs (Fig. S2F), CXCL1/KC and CXCL5/LIX were decreased in BALF and lung homogenates (Fig. S2G-J) in Nlrp6$^{-/-}$ mice as compared to WT mice. Altogether, our results demonstrate that NLRP6 is central to pulmonary inflammatory responses to CS exposure. Since NLRP6 plays comparable roles in pulmonary inflammation and remodeling upon acute (1w) and subchronic (6w)-CS exposure in mice, we then preferentially performed acute exposure to investigate the mechanism of NLRP6-mediated lung inflammation.

NLRP6 expression in radioresistant cells is necessary for neutrophil influx and IL-1β production

In order to investigate the cellular source of NLRP6 involved in acute CS-induced inflammation, we addressed its respective contribution in bone marrow (BM)-derived versus resident cells using bone marrow transplantation. WT (CD45.1) and Nlrp6$^{-/-}$ (CD45.2) recipient mice were sub-lethally irradiated (2 x 5.5 Gy, 3h apart) and reconstituted with either WT or Nlrp6$^{-/-}$ BM cells. CS-induced neutrophil recruitment (Fig. 2A) and MPO levels (Fig. 2B) in BALF were significantly reduced in Nlrp6 deficient recipient mice (WT>Nlrp6$^{-/-}$ and Nlrp6$^{-/-}$>Nlrp6$^{-/-}$) but not in WT recipient mice (Nlrp6$^{-/-}$>WT and WT>WT). In addition, we observed a trend for decreased lung IL-1β levels in Nlrp6 deficient recipient mice (Fig. 2C). These data indicate that NLRP6-dependent neutrophil influx, MPO and potentially IL-1β productions in response to acute CS-exposure, are dependent on Nlrp6 expression by non-immune/radioresistant cells rather than BM-derived immune cells. In addition, while not significantly decreased in Nlrp6$^{-/-}$>Nlrp6$^{-/-}$ and Nlrp6$^{-/-}$>WT mice, lung CXCL1 expression seems to display a non-negligible BM-derived contribution (Fig. 2D). In addition, remodeling factors MMP-9 (Fig. 2E) and TIMP-1 (Fig. 2F) were decreased in Nlrp6$^{-/-}$>WT, WT>Nlrp6$^{-/-}$ and Nlrp6$^{-/-}$>Nlrp6$^{-/-}$ mice in comparison to WT> WT mice suggesting an NLRP6-dependent production in both BM-derived and resident cells. As a whole, these data indicate that BALF neutrophilic influx upon CS exposure depends on NLRP6 expression in resident cells.

Acute CS-exposure induces NLRP6 expression in airway epithelial cells

Since we observed that neutrophil influx upon CS-exposure depends on NLRP6 expression in resident cells (Fig. 2, A and B), we investigated whether NLRP6 is expressed in epithelial cells.

We first isolated trachea epithelial cells from Wild type mice and performed air liquid interface (ALI) in *in vitro* culture. We analyzed Nlrp6 mRNA basal expression by specific *Nlrp6* RT-PCR and observed a 148 bp band corresponding to expected Nlrp6 cDNA size (Fig. 3A). Epithelial cells markers (*Krt8* and *Ocln1*) were quantified by qPCR, confirming basal Nlrp6 expression in trachea epithelial cells **(**Fig. 3B**)**. Sequencing this amplified cDNA, we identified Nlrp6 sequence (Fig. 3C).Then we exposed NLRP6-FLAG-IRES-GFP reported mice and WT C56BL/6 mice to CS or air during 4 days. Performing FLAG-specific immunohistochemistry analysis of lung sections, we observed increased FLAG expression in bronchial cells from CS-exposed mice in comparison to air-exposed mice and no FLAG expression in WT C56BL/6 CS-exposed mice (Fig. 3D). These results indicate that acute CS-exposure enhances NLRP6 expression in bronchial airway epithelial cells in mice.

Specific NLRP6 deficiency in lung cells dampens pulmonary inflammation to CS

To confirm that NLRP6 expressed in lung cells may control airway and lung inflammation, we generated mice deficient for Nlrp6 specifically in aquaporin-expressing lung epithelium ($Nlrp6^{fl/fl}$ $Acid^{+/CRE}$) as well as their control littermate mice ($Nlrp6^{fl/fl}$ $Acid^{+/+}$) and exposed them to CS for 4 days. We show that $Nlrp6^{fl/fl}$ $Acid^{+/Cre}$ mice displayed reduced BALF total cells influx and in particular neutrophil counts and MPO levels in comparison to $Nlrp6^{fl/fl}$ $Acid^{+/+}$ littermate mice (Fig. 4, A and B). CXCL1 (Fig. 4, C and D) and CXCL5 (Fig. 4, E and F) levels were very significantly decreased in the BALF whereas only a tendency was observed in the lungs of CS-exposed $Nlrp6^{fl/fl}$ $Acid^{+/Cre}$ as shown above in total $Nlrp6^{-/-}$ mice. Altogether, our findings indicate that NLRP6 expression in lung cells controls pulmonary inflammation to CS exposure.

NLRP6 inflammasome controls pulmonary inflammation and remodeling to CS exposure

Since part of NLRP6 function relies on inflammasome activation, we investigated the role of inflammasome-related molecules ASC, Casp-1 and Casp-11. After 4 days CS exposure, we confirmed that BALF neutrophil numbers (Fig. 5A) and MPO levels (Fig. 5B), CXCL1 and CXCL5 levels in BALF and lungs (Fig. 5C-F), were dramatically reduced in $Asc^{-/-}$ or $Casp\text{-}1/11^{-/-}$ similarly than observed in $Nlrp6^{-/-}$ mice suggesting an inflammasome-dependent function of NLRP6 in neutrophilic inflammation.

Since we observed that resident pulmonary cells play an important role in NLRP6 inflammasome-mediated airway inflammation to CS (Fig. 2), we analyzed in more details the role of CXCL5, a neutrophilic chemokine essentially produced by airway epithelial cells. CXCL5 and which is crucial for lung inflammation to CS exposure [11; 12; 38; 39]. We report that CXCL5 levels, as well as CXCL1, were decreased in both BALF (Fig. 5, C and E) and lungs (Fig. 5, D and F) of $Asc^{-/-}$ or $Casp\text{-}1/11^{-/-}$ mice indicating that Casp-1/11-dependent inflammasome formation contributes to chemokine production.

To confirm that CXCL5 essentially produced by airway epithelial cells, is a crucial chemokine in CS-induced pulmonary inflammation [11; 12; 38; 39], WT mice were intraperitoneally treated with CXCL5 neutralizing antibodies. A very significant decrease in BALF CXCL5 levels after anti-CXCL5 antibody treatment indicated efficient neutralization in the BALF (Fig. S3A). Of note, we also observed decreased BALF CXCL1 levels suggesting that CXCL5 secretion indirectly influences CXCL1 in CS-exposed mice (Fig. S3B), supposedly by decreasing neutrophil-mediated macrophage activity. In line with decreased neutrophilic chemokines, BALF total cells, neutrophil numbers (Fig. S3, C and D), and MPO levels (Fig. S3E) were reduced after CXCL5 blockade. Conversely, airway instillation of recombinant CXCL5 (rCXCL5) in CS-

exposed Nlrp6$^{-/-}$ mice was sufficient to restore most of CS-induced BALF neutrophil influx and MPO levels (Fig. S3, F and G), demonstrating that CXCL5 is a major neutrophil chemokine in CS-induced inflammation.

Oral antibiotic treatment decreases pulmonary inflammation to CS

Since NLRP6 was shown to control gut microbiota composition and inflammation with dysbiosis in Nlrp6$^{-/-}$ mice [25; 26; 27; 41; 42] we hypothesized that gut microbiota from Nlrp6$^{-/-}$ mice could influence pulmonary inflammation through a gut to lung axis. In that context, we analyzed whether microbiota perturbation may disturb CS-induced lung inflammatory response and in particular neutrophilic chemokine secretion and neutrophil influx. We treated WT mice with broad-spectrum antibiotics ad libidum in drinking water for two weeks and exposed them to CS during the last 4 days (Fig. 6A). Antibiotic treatment resulted in a drastic increased of caecum size (Fig. 6B), as previously observed or in germ-free mice, as well as significant body weight loss (Fig. 6C). Total cell counts (Fig. 6D), neutrophils percentage and numbers (Fig. 6, E and F) in BALF, MPO (Fig. 6, G and H), CXCL1 (Fig. 6I and J), CXCL5 (Fig. 6K and L) levels were decreased in BALF and lung homogenates. In addition, IL-1β levels in the lungs (Fig. 6M), MMP-9 (Fig. 6, N and O) and TIMP-1 (Fig. 6, P and Q) levels in BALF and lungs were attenuated. These results show that whole body bacterial depletion in WT mice impairs pulmonary inflammation upon CS exposure and recapitulates our results observed in Nlrp6$^{-/-}$ mice. The data suggest that gut microbiota is involved in CS-induced lung inflammation.

Impaired CS-induced airway inflammation in Nlrp6$^{-/-}$ mice is transferable to wild type mice by cohousing

To decipher whether gut microbiota from Nlrp6$^{-/-}$ influences pulmonary inflammation, WT mice were co-housed (WT CH) for 3 months with Nlrp6$^{-/-}$ mice (Nlrp6$^{-/-}$ CH). Single-housed WT (WT SH) and Nlrp6$^{-/-}$ (Nlrp6$^{-/-}$ SH) mice were used as controls. Then, mice were exposed to air or CS for 4 days (Fig. 7A) and their gut microbiota composition analyzed using unbiased 16S ribosomal RNA (rRNA) gene high throughput sequencing. As expected, the dominant phyla were represented by Firmicutes, Bacteroidetes, Proteobacteria and Actinobacteria and differences appeared comparing WT versus Nlrp6$^{-/-}$ mice (Fig. S4 and S5). No significant change in alpha diversity was observed in intestinal microbiota among the different mouse groups (Fig. S6). However, principal component analysis (PCA) of beta diversity showed sharp differences comparing WT SH and Nlrp6$^{-/-}$ SH mice, which were abrogated upon cohousing. This confirms differences is gut microbiota composition between WT and Nlrp6$^{-/-}$ mice as previously reported [25; 41; 43; 44]. Indeed, WT SH and Nlrp6$^{-/-}$ SH mice exposed to air (Fig. 7B) or to CS (Fig. 7C) cluster separately on the PC1 axis while the cohoused clusters became indistinguishable. Using LDA Effect Size (LEfSe) [45], specific differences stand out in gut microbiota composition between WT and Nlrp6$^{-/-}$ mice exposed to air or CS (Fig. S4, S5 and S7). These differences mostly disappear upon co-housing (Fig. S8) demonstrating the efficacy of the microbiota transfer by this method.

In addition, analysis of gut microbiota from single-housed WT or Nlrp6$^{-/-}$ mice exposed to air or to CS revealed that CS exposure affects intestinal microbiota composition in both WT (Fig. 7D) and Nlrp6$^{-/-}$ (Fig. 7E) mice indicating that CS airway exposure may influence gut homeostasis and/or inflammation. However, CS-driven gut microbiota alterations were distinct in WT versus

Nlrp6$^{-/-}$ (Fig. S7) suggesting possible connections linking CS, gut microbiota and NLRP6-mediated airway inflammation. In line with this hypothesis, Nlrp6$^{-/-}$ phenotype characterized by decreased cell recruitment (Fig. 7F) and in particular neutrophil influx (Fig. 7G) as well as BALF CXCL1 (Fig. 7H) and CXCL5 (Fig. 7I) levels was transferred to WT mice upon cohousing. These results indicate that intestinal microbiota influences CS-induced airway inflammation. Noteworthy, we observed that total cells (Fig. 7F), especially neutrophils influx (Fig. 7G), CXCL1 (Fig. 7H) and CXCL5 (Fig. 7I) secretions into the BALF remained low in Nlrp6$^{-/-}$ cohoused with WT mice (Nlrp6 CH), indicating that microbiota from Nlrp6$^{-/-}$ mice displays a dominant effect. These results highlight differences in gut microbiota composition between WT and Nlrp6$^{-/-}$ mice and show that gut microbiota from Nlrp6$^{-/-}$ mice limits airway inflammation to CS exposure.

Oral transplantation of WT germ-free mice with fecal microbiota from Nlrp6$^{-/-}$ mice attenuated CS exposure-induced lung inflammation

To confirm that gut microbiota regulates airway inflammation to CS exposure in an NLRP6-dependent manner, we colonized germ-free (GF) WT mice (WT^{GF}) with fecal microbiota obtained from WT or Nlrp6$^{-/-}$ mice bred in the same EOPS mouse facility. Transplanted mice were maintained in isolators for 4 weeks to allow microbiota reconstitution and immune system maturation. Following one week of acclimation in a conventional breeding facility, mice were exposed to CS for 4 days (Fig.8A). While GF mice are unable to mount proper inflammatory response [43], we observed that reconstitution of WT^{GF} mice with WT microbiota (WT>WT^{GF}) allows a normal lung inflammatory response to CS with CXCL5 secretion in the bronchoalveolar space (Fig. 8, B-F). In contrast, WT^{GF} mice colonized with microbiota from Nlrp6$^{-/-}$ mice (Nlrp6$^{-/-}$>WT^{GF}) displayed decreased cellular influx in BALF (Fig. 8B), in particular of neutrophil (Fig.

8C) associated with decreased MPO (Fig. 8D), CXCL1 (Fig. 8E) and CXCL5 (Fig. 8F) levels in BALF as compared to WT>WT^{GF} mice. These results confirm that gut microbiota shapes lung inflammation and that gut microbiota from Nlrp6$^{-/-}$ mice negatively regulates lung inflammation upon acute CS exposure.

Discussion

NOD-like receptor family pyrin domain containing (NLRP)6 inflammasome was shown to regulate microbiota homeostasis as well as antibacterial and antiviral immunity in the intestine [24; 25; 26; 27; 28; 41]. However, the role of this multifaceted immune sensor in the lungs remains poorly understood. Studies showed that NLRP6 controls neutrophil recruitment and function during pulmonary bacterial infection [29; 30; 46; 47; 48] but its involvement in the context of sterile lung injury remains elusive. We chose to understand early inflammation mechanisms because acute inflammation repetition often lead to chronicity and lung pathology. In addition, episodes of acute inflammatory exacerbations due to bacterial infections, frequently observed in COPD patients, are associated with dramatic increased pathology severity. Therefore, a better characterization of the mechanisms of acute phases of inflammation appears crucial.

We demonstrate that NLRP6 positively controls both pulmonary inflammation and remodeling to cigarette smoke exposure. Nlrp6 deficient mice (Nlrp6$^{-/-}$) displayed drastic reduction of airway cell recruitment particularly neutrophils, macrophages and lymphocytes and attenuated lung tissue inflammation in comparison to wild type (WT) mice. Interestingly, NLRP6 contribution is likely context-dependent as it was shown to negatively regulate pulmonary host defense after gram-positive bacterial infection through neutrophil influx modulation [29]. COPD patients often suffer from disease exacerbations due to bacterial infections and despite strong neutrophil-driven

554 inflammation, these cells are largely ineffective leading to impaired bacterial clearance [49; 50;
555 51]. A possibility is that NLRP6 favors chronic detrimental neutrophilic inflammation but
556 suppresses anti-bacterial immunity. If true, targeting NLRP6 in COPD patients might be
557 beneficial by preventing chronic inflammation and bacterial infection-driven disease
558 exacerbation. This hypothesis could be tested in COPD exacerbation models by infecting
559 chronically CS exposed mice to bacteria such as Streptococcus pneumonia or Haemophilus
560 influenza.
561 Our data demonstrate for the first time that NLRP6 is a sensor of lung injury here induced by CS
562 but possibly by other chemicals and toxics, opening new investigation fields. We verified that
563 mouse genetic background and/or housing were not responsible for the difference in
564 inflammatory response to CS observed using $Nlrp6^{+/+}$ and $Nlrp6^{-/-}$ littermate mice and observed
565 similar decreased pulmonary inflammation in $Nlrp6^{-/-}$ mice in comparison to $Nlrp6^{+/+}$ littermate.
566 We provide evidence that NLRP6 expression in radioresistant cells positively regulates CS-
567 mediated airway neutrophil inflammation. Our results show that NLRP6 is expressed in tracheal
568 and lung epithelial cells and indicate that acute CS-exposure enhances NLRP6 expression in
569 airway epithelial cells in mice. Although much less than in the intestine, NLRP6 was shown
570 expressed in the lungs in epithelial cells and tissue infiltrating neutrophils and macrophages after
571 bacterial infection of human or mice [29; 30; 46; 47; 48]).
572 Then, using mice deficient for Nlrp6 specifically in aquaporin-expressing lung cells ($Nlrp6^{fl/fl}$
573 $Acid^{+/CRE}$) and their control littermate ($Nlrp6^{fl/fl}$ $Acid^{+/+}$) we demonstrate that NLRP6 expressed
574 in lung controls neutrophilic airway and lung inflammation in response to acute CS exposure.
575 We confirmed that CXCL5, a neutrophilic chemokine essentially produced by airway epithelial
576 cells, is a crucial chemokine in CS-induced pulmonary inflammation [11; 13; 39; 52; 53]. In
577 addition, exogenous recombinant CXCL5 was sufficient to restore neutrophilic inflammation in

578 Nlrp6$^{-/-}$ mice suggesting that NLRP6 expressed in airway epithelial cells plays a key role in
579 CXCL5 production and secretion and leads to neutrophil recruitment and airways inflammation.
580 We report a new role for the NLRP6 inflammasome in pulmonary inflammation to CS exposure
581 through production of the neutrophilic chemokine CXCL1/KC and CXCL5/LIX leading to
582 neutrophils influx and airway inflammation. NLRP6 expression and function in airway epithelial
583 cells highlights active contribution of tissue constitutive cells in pulmonary inflammation as
584 supported recently [16; 17]. In addition, the NLRP6, ASC, Casp-1 and/or Casp-11
585 inflammasome-related proteins contribute to CS-induced pulmonary inflammation. CS-exposure
586 induced NLRP6 expression in AEC suggesting the formation of the NLRP6 inflammasome in
587 these cells. We recently reported that CS-exposure induces NLRP3-dependent caspase-1
588 activation in bronchoalveolar space macrophages and NLRP3-dependent gasdermin D activation
589 in both bronchoalveolar space macrophages and bronchial epithelial cells [54]. This indicate that
590 both NLRP3 and NLRP6 inflammasomes are involved in CS-induced pulmonary inflammation.
591 However, inflammasome-independent role of NLRP6 was reported in intestinal epithelial cells
592 [28]. Indeed NLRP6 was showed to control enteric virus infection through its binding to viral
593 RNA via the RNA helicase Dhx15 and interacted with mitochondrial antiviral signaling protein
594 to induce type I/III interferons and IFN-stimulated genes [28]. Even if we observed a similar
595 reduction in inflammation in the absence of NLRP6, ASC or Casp1/11, we cannot exclude that
596 NLRP6 could play a role independently of inflammasome via unknown partners.
597 Here we hypothesized that gut microbiota from Nlrp6$^{-/-}$ mice could influence pulmonary
598 inflammation through a gut to lung axis. We showed that whole body bacterial depletion in WT
599 mice impairs pulmonary inflammation upon CS exposure and recapitulates our results observed
600 in Nlrp6$^{-/-}$ mice. Interestingly, Nlrp6$^{-/-}$ mice presented defective mucus secretion and intestinal
601 barrier, reduced control of colonic host-microbial interface and microbiota dysbiosis [25; 26].

These results were challenged when Nlrp6$^{+/+}$ and Nlrp6$^{-/-}$ littermate were used, both displaying intact mucus layer [55]. However, *ex vivo* LPS-induced mucus secretion was shown to be defective in intestinal goblet cells of colonic tissue from Nlrp6$^{-/-}$ mice in comparison to Nlrp6$^{+/+}$ littermate [55].

Importantly we report for the first time the existence of an NLRP6-dependent gut to lung axis controlling pulmonary inflammation to CS-induced injury. Cohousing and fecal transplantation experiments both revealed that Nlrp6$^{-/-}$ gut microbiota transfer to WT mice impedes pulmonary inflammation in response to CS. During cohousing or fecal transplantation, metabolites generated by Nlrp6$^{-/-}$ gut microbiota upon CS-exposure may inhibit NLRP6 in airway epithelial cells of WT mice. In addition, antibiotic-mediated microbiota depletion indicates that microbiome is required for efficient lung immunity. While antibiotic treatment probably affects both gut and lung microbiota, these data suggest that the predominant gut microbiota is necessary for CS-induced lung inflammation through NLRP6 activation and subsequent lung inflammation. Lung microbiota composition analysis is difficult to perform because of the weak amount of bacteria. However, we believe that as shown, NLRP6-dependent perturbation of the gut microbiome may generate specific metabolites or compounds [43; 56] that might modulate NLRP6 inflammasome activation in lung.

Our study supports evidence of an altered gut microbiota between WT and Nlrp6$^{-/-}$ mice as previously reported [25; 41; 43; 44]. Two studies suggested that NLRP6 inflammasome does not shape commensal gut microbiota composition by analyzing gut microbiota phylogenetic after DSS-induced colitis of ASC-deficient mice [57; 58]. However, two other laboratories reported that littermate breeding led to the development of distinct microbiome compositions in NLRP6 inflammasome-deficient mice housed in two different facilities [27; 43].

In addition, two independent groups showed that NLRP6 deficiency lead to impaired intestinal mucus secretion, disrupted mucus barrier and mucosal surface invasion by enteric pathogens and finally to dysbiosis [25; 26] but this was discussed by another group [55]. These seemingly conflicting results might be explained by differences in microbiome compositions between laboratories. Indeed, familial transmission was shown to significantly influence microbiota composition in conventionally housed Nlrp6$^{-/-}$ mice. In addition, introduction of potential pathobionts revealed effects of Nlrp6 deficiency on gut microbiome and increased abundance of pathobionts was observed in Nlrp6$^{-/-}$ mice indicating that Nlrp6$^{-/-}$ microbiota depends on community structure [42]. Moreover, littermate approach has been coupled with generation of germ-free mice. De novo dysbiosis was observed in spontaneous recolonization of germ-free NLRP6$^{-/-}$ mice [43] as well as after fecal transfer of diverse microbiomes in germ-free NLRP6$^{-/-}$ mice, as compared to germ-free WT mice [27; 42; 43].

Our results obtained after cohousing or fecal transplantation experiments, or antibiotics treatments demonstrate that airway exposure to CS significantly alters gut microbiota composition and hence may influence gut homeostasis and/or inflammation. These observations are in line with data showing increased risk of smokers and COPD patients to develop intestinal diseases and support the notion of a complex interplay between environmental factors, gut microbiota and organ disease [59; 60]. Epidemiological evidence linked gut dysbiosis and COPD [61; 62]. Interestingly, some specific changes we observed in gut microbiota of CS-exposed Nlrp6$^{-/-}$ mice are inversely correlated to faecal microbiome taxonomic indicators described in COPD patients. For example, upon CS-exposure Clostridia are increased in gut microbiota of Nlrp6$^{-/-}$ mice in comparison to WT mice (Fig. S5) but depleted in faecal microbiome of COPD patients in comparison to healthy subject. Inversely Bifidobacteriaceae are decreased in gut microbiota of Nlrp6$^{-/-}$ mice whereas increased in faecal microbiome of COPD patients [63].

In addition, severe COPD was associated with reduced sputum microbiota diversity [64] and lung microbiome dynamics during stability and exacerbation, influences COPD pathogenicity [65; 66]. It is likely that the lung microbiota may be influenced by CS exposure in our mouse model as shown in COPD patients [66]. In particular, during infection-triggered acute COPD exacerbations, pathogens promote lung microbiota dysbiosis that may favor intestinal diseases, pointing to the existence of a bidirectional connection between the lungs and the gut in COPD [67]. Altered lung microbiota in Nlrp6$^{-/-}$ mice could interfere with host defense against lung infection in particular triggered by Streptococcus pneumonia (*S.p.*) and frequently associated with COPD exacerbation [68]. However, NLRP6 was shown to negatively regulate inflammation to *S.p.* [31; 48] or to Staphylococcus aureus infections [29] suggesting a beneficial role of Nlrp6 depletion or inhibition in these secondary infections. However, NLRP6 might exhibit detrimental functions in other infection settings. We show that both NLRP6 expression in lung and gut controls CS-induced pulmonary inflammation. Gut microbiota shaped by NLRP6 expressed in gut, regulates pulmonary inflammation to CS probably via circulating microbiota-derived metabolites [69]. In addition to gut metabolites, gut-microbiota-derived components can also modulate lung inflammation, such as *lipoteichoic acid (LTA)*, a major constituent of the cell wall of gram-positive bacteria that was shown to induce inflammation through NLRP6 sensing in wild-type mice but not in Nlrp6$^{-/-}$ mice [70]. As a whole, we report new data supporting important NLRP6 functions in basal and pathological lung settings that could be translated to the clinic following preclinical validations. Gut microbiota-derived metabolites or components might represent biomarkers present in the blood of COPD patients [43; 71]. In addition, this study uncovers NLRP6 as a new target for the development of potential therapeutic strategies against COPD by specific inhibition of NLRP6 or gut microbiota transfer approaches might be useful in the treatment of COPD.

Author contributions

MN, MF, SHM, MS, FS, NR and AG performed the experiments.

MN, NR, AG, PG, HS and IC conceived the experiments and analyzed the data.

MLB supervised mouse breeding.

LA, MC provided mouse strains.

JVS provided antibodies.

MN, NR, MLB, BR, VFJQ, FT, PG, HS and IC discussed the results.

MN, NR, BR, AG, HA and IC wrote the manuscript.

IC, FT, HS, PG and VJFQ provided funding and IC overall supervision of this study.

Acknowledgments

We are grateful to Hélène Bouscayrol from the Oncology-radiotherapy Department at Regional Hospital in Orleans, for access to the animal irradiator and Isabelle Hermelin for the possibility to obtain vancomycin from the CHU pharmacy. We also thank Tamara Durand, Nathalie Froux and Elsa Ramon from TAAM for stool collection and animal gavage. The graphical abstract has been created thanks to adapted items from Servier Medical ART.

Declaration of Interests

All authors declare no competing interests.

References

[1] P.J. Barnes, Mediators of chronic obstructive pulmonary disease. Pharmacol Rev 56 (2004) 515-48.

[2] A. Agusti, B.R. Celli, G.J. Criner, D. Halpin, A. Anzueto, P. Barnes, J. Bourbeau, M.K. Han, F.J. Martinez, M. Montes de Oca, K. Mortimer, A. Papi, I. Pavord, N. Roche, S. Salvi, D.D. Sin, D. Singh, R. Stockley, M.V. Lopez Varela, J.A. Wedzicha, and C.F. Vogelmeier, Global Initiative for Chronic Obstructive Lung Disease 2023 Report: GOLD Executive Summary. Am J Respir Crit Care Med 207 (2023) 819-837.

[3] R.A. Pauwels, and K.F. Rabe, Burden and clinical features of chronic obstructive pulmonary disease (COPD). Lancet 364 (2004) 613-20.

[4] J.D. Morrow, B. Make, E. Regan, M. Han, C.P. Hersh, R. Tal-Singer, J. Quackenbush, A.M.K. Choi, E.K. Silverman, and D.L. DeMeo, DNA Methylation is Predictive of Mortality in Current and Former Smokers. Am J Respir Crit Care Med (2020).

[5] C.A. Brandsma, M. Van den Berge, T.L. Hackett, G. Brusselle, and W. Timens, Recent advances in chronic obstructive pulmonary disease pathogenesis: from disease mechanisms to precision medicine. J Pathol (2019).

[6] G.G. Brusselle, G.F. Joos, and K.R. Bracke, New insights into the immunology of chronic obstructive pulmonary disease. Lancet 378 (2011) 1015-26.

[7] P.J. Barnes, Inflammatory mechanisms in patients with chronic obstructive pulmonary disease. J Allergy Clin Immunol 138 (2016) 16-27.

[8] P.J. Barnes, Cellular and molecular mechanisms of asthma and COPD. Clin Sci (Lond) 131 (2017) 1541-1558.

[9] A. Butler, G.M. Walton, and E. Sapey, Neutrophilic Inflammation in the Pathogenesis of Chronic Obstructive Pulmonary Disease. COPD 15 (2018) 392-404.

[10] I. Clark-Lewis, B. Dewald, M. Loetscher, B. Moser, and M. Baggiolini, Structural requirements for interleukin-8 function identified by design of analogs and CXC chemokine hybrids. J Biol Chem 269 (1994) 16075-81.

[11] S. Jeyaseelan, R. Manzer, S.K. Young, M. Yamamoto, S. Akira, R.J. Mason, and G.S. Worthen, Induction of CXCL5 during inflammation in the rodent lung involves activation of alveolar epithelium. Am J Respir Cell Mol Biol 32 (2005) 531-9.

[12] J.N. Vanderbilt, E.M. Mager, L. Allen, T. Sawa, J. Wiener-Kronish, R. Gonzalez, and L.G. Dobbs, CXC chemokines and their receptors are expressed in type II cells and upregulated following lung injury. Am J Respir Cell Mol Biol 29 (2003) 661-8.

[13] Y. Liu, J. Mei, L. Gonzales, G. Yang, N. Dai, P. Wang, P. Zhang, M. Favara, K.C. Malcolm, S. Guttentag, and G.S. Worthen, IL-17A and TNF-alpha exert synergistic effects on

736 expression of CXCL5 by alveolar type II cells in vivo and in vitro. J Immunol 186 (2011)
737 3197-205.
738 [14] J.B. Smith, L.E. Rovai, and H.R. Herschman, Sequence similarities of a subgroup of CXC
739 chemokines related to murine LIX: implications for the interpretation of evolutionary
740 relationships among chemokines. J Leukoc Biol 62 (1997) 598-603.
741 [15] L.E. Rovai, H.R. Herschman, and J.B. Smith, The murine neutrophil-chemoattractant
742 chemokines LIX, KC, and MIP-2 have distinct induction kinetics, tissue distributions, and
743 tissue-specific sensitivities to glucocorticoid regulation in endotoxemia. J Leukoc Biol 64
744 (1998) 494-502.
745 [16] M.J. Holtzman, D.E. Byers, J. Alexander-Brett, and X. Wang, The role of airway epithelial
746 cells and innate immune cells in chronic respiratory disease. Nat Rev Immunol 14 (2014)
747 686-98.
748 [17] J.A. Whitsett, and T. Alenghat, Respiratory epithelial cells orchestrate pulmonary innate
749 immunity. Nat Immunol 16 (2015) 27-35.
750 [18] E. Doz, N. Noulin, E. Boichot, I. Guenon, L. Fick, M. Le Bert, V. Lagente, B. Ryffel, B.
751 Schnyder, V.F. Quesniaux, and I. Couillin, Cigarette smoke-induced pulmonary
752 inflammation is TLR4/MyD88 and IL-1R1/MyD88 signaling dependent. J Immunol 180
753 (2008) 1169-78.
754 [19] I. Couillin, V. Vasseur, S. Charron, P. Gasse, M. Tavernier, J. Guillet, V. Lagente, L. Fick,
755 M. Jacobs, F.R. Coelho, R. Moser, and B. Ryffel, IL-1R1/MyD88 signaling is critical for
756 elastase-induced lung inflammation and emphysema. J Immunol 183 (2009) 8195-202.
757 [20] L. Broderick, D. De Nardo, B.S. Franklin, H.M. Hoffman, and E. Latz, The inflammasomes
758 and autoinflammatory syndromes. Annu Rev Pathol 10 (2015) 395-424.
759 [21] F. Martinon, and L.H. Glimcher, Gout: new insights into an old disease. J Clin Invest 116
760 (2006) 2073-5.
761 [22] Y. Ataman-Onal, S. Munier, A. Ganee, C. Terrat, P.Y. Durand, N. Battail, F. Martinon, R.
762 Le Grand, M.H. Charles, T. Delair, and B. Verrier, Surfactant-free anionic PLA
763 nanoparticles coated with HIV-1 p24 protein induced enhanced cellular and humoral
764 immune responses in various animal models. J Control Release 112 (2006) 175-85.
765 [23] E. Elinav, T. Strowig, J. Henao-Mejia, and R.A. Flavell, Regulation of the antimicrobial
766 response by NLR proteins. Immunity 34 (2011) 665-79.
767 [24] S. Normand, A. Delanoye-Crespin, A. Bressenot, L. Huot, T. Grandjean, L. Peyrin-Biroulet,
768 Y. Lemoine, D. Hot, and M. Chamaillard, Nod-like receptor pyrin domain-containing
769 protein 6 (NLRP6) controls epithelial self-renewal and colorectal carcinogenesis upon
770 injury. Proc Natl Acad Sci U S A 108 (2011) 9601-6.
771 [25] M. Wlodarska, C.A. Thaiss, R. Nowarski, J. Henao-Mejia, J.P. Zhang, E.M. Brown, G.
772 Frankel, M. Levy, M.N. Katz, W.M. Philbrick, E. Elinav, B.B. Finlay, and R.A. Flavell,
773 NLRP6 inflammasome orchestrates the colonic host-microbial interface by regulating
774 goblet cell mucus secretion. Cell 156 (2014) 1045-59.
775 [26] G.M. Birchenough, E.E. Nystrom, M.E. Johansson, and G.C. Hansson, A sentinel goblet cell
776 guards the colonic crypt by triggering Nlrp6-dependent Muc2 secretion. Science 352
777 (2016) 1535-42.
778 [27] S.S. Seregin, N. Golovchenko, B. Schaf, J. Chen, K.A. Eaton, and G.Y. Chen, NLRP6
779 function in inflammatory monocytes reduces susceptibility to chemically induced
780 intestinal injury. Mucosal Immunol (2016).

[28] P. Wang, S. Zhu, L. Yang, S. Cui, W. Pan, R. Jackson, Y. Zheng, A. Rongvaux, Q. Sun, G. Yang, S. Gao, R. Lin, F. You, R. Flavell, and E. Fikrig, Nlrp6 regulates intestinal antiviral innate immunity. Science 350 (2015) 826-30.
[29] L. Ghimire, S. Paudel, L. Jin, P. Baral, S. Cai, and S. Jeyaseelan, NLRP6 negatively regulates pulmonary host defense in Gram-positive bacterial infection through modulating neutrophil recruitment and function. PLoS Pathog 14 (2018) e1007308.
[30] S. Cai, S. Paudel, L. Jin, L. Ghimire, C.M. Taylor, N. Wakamatsu, D. Bhattarai, and S. Jeyaseelan, NLRP6 modulates neutrophil homeostasis in bacterial pneumonia-derived sepsis. Mucosal Immunol 14 (2021) 574-584.
[31] D. Xu, X. Wu, L. Peng, T. Chen, Q. Huang, Y. Wang, C. Ye, Y. Peng, D. Hu, and R. Fang, The Critical Role of NLRP6 Inflammasome in Streptococcus pneumoniae Infection In Vitro and In Vivo. Int J Mol Sci 22 (2021).
[32] S. Mariathasan, K. Newton, D.M. Monack, D. Vucic, D.M. French, W.P. Lee, M. Roose-Girma, S. Erickson, and V.M. Dixit, Differential activation of the inflammasome by caspase-1 adaptors ASC and Ipaf. Nature 430 (2004) 213-8.
[33] K. Kuida, J.A. Lippke, G. Ku, M.W. Harding, D.J. Livingston, M.S. Su, and R.A. Flavell, Altered cytokine export and apoptosis in mice deficient in interleukin-1 beta converting enzyme. Science 267 (1995) 2000-3.
[34] P. Flodby, Z. Borok, A. Banfalvi, B. Zhou, D. Gao, P. Minoo, D.K. Ann, E.E. Morrisey, and E.D. Crandall, Directed expression of Cre in alveolar epithelial type 1 cells. Am J Respir Cell Mol Biol 43 (2010) 173-8.
[35] X. Chen, Y. Wang, Q. Li, S. Tsai, A. Thomas, J.A. Shizuru, and T.M. Cao, Pathways analysis of differential gene expression induced by engrafting doses of total body irradiation for allogeneic bone marrow transplantation in mice. Immunogenetics 65 (2013) 597-607.
[36] B. Lamas, M.L. Richard, V. Leducq, H.P. Pham, M.L. Michel, G. Da Costa, C. Bridonneau, S. Jegou, T.W. Hoffmann, J.M. Natividad, L. Brot, S. Taleb, A. Couturier-Maillard, I. Nion-Larmurier, F. Merabtene, P. Seksik, A. Bourrier, J. Cosnes, B. Ryffel, L. Beaugerie, J.M. Launay, P. Langella, R.J. Xavier, and H. Sokol, CARD9 impacts colitis by altering gut microbiota metabolism of tryptophan into aryl hydrocarbon receptor ligands. Nat Med 22 (2016) 598-605.
[37] J.G. Caporaso, J. Kuczynski, J. Stombaugh, K. Bittinger, F.D. Bushman, E.K. Costello, N. Fierer, A.G. Pena, J.K. Goodrich, J.I. Gordon, G.A. Huttley, S.T. Kelley, D. Knights, J.E. Koenig, R.E. Ley, C.A. Lozupone, D. McDonald, B.D. Muegge, M. Pirrung, J. Reeder, J.R. Sevinsky, P.J. Turnbaugh, W.A. Walters, J. Widmann, T. Yatsunenko, J. Zaneveld, and R. Knight, QIIME allows analysis of high-throughput community sequencing data. Nat Methods 7 (2010) 335-6.
[38] G. Balamayooran, S. Batra, S. Cai, J. Mei, G.S. Worthen, A.L. Penn, and S. Jeyaseelan, Role of CXCL5 in leukocyte recruitment to the lungs during secondhand smoke exposure. Am J Respir Cell Mol Biol 47 (2012) 104-11.
[39] J.K. Nikota, P. Shen, M.C. Morissette, K. Fernandes, A. Roos, D.K. Chu, N.G. Barra, Y. Iwakura, R. Kolbeck, A.A. Humbles, and M.R. Stampfli, Cigarette smoke primes the pulmonary environment to IL-1alpha/CXCR-2-dependent nontypeable Haemophilus influenzae-exacerbated neutrophilia in mice. J Immunol 193 (2014) 3134-45.
[40] L.J. Seys, F.M. Verhamme, A. Schinwald, H. Hammad, D.M. Cunoosamy, C. Bantsimba-Malanda, A. Sabirsh, E. McCall, L. Flavell, R. Herbst, S. Provoost, B.N. Lambrecht, G.F.

Joos, G.G. Brusselle, and K.R. Bracke, Role of B Cell-Activating Factor in Chronic Obstructive Pulmonary Disease. Am J Respir Crit Care Med 192 (2015) 706-18.
[41] E. Elinav, T. Strowig, A.L. Kau, J. Henao-Mejia, C.A. Thaiss, C.J. Booth, D.R. Peaper, J. Bertin, S.C. Eisenbarth, J.I. Gordon, and R.A. Flavell, NLRP6 inflammasome regulates colonic microbial ecology and risk for colitis. Cell 145 (2011) 745-57.
[42] E.J.C. Galvez, A. Iljazovic, A. Gronow, R. Flavell, and T. Strowig, Shaping of Intestinal Microbiota in Nlrp6- and Rag2-Deficient Mice Depends on Community Structure. Cell Rep 21 (2017) 3914-3926.
[43] M. Levy, C.A. Thaiss, D. Zeevi, L. Dohnalova, G. Zilberman-Schapira, J.A. Mahdi, E. David, A. Savidor, T. Korem, Y. Herzig, M. Pevsner-Fischer, H. Shapiro, A. Christ, A. Harmelin, Z. Halpern, E. Latz, R.A. Flavell, I. Amit, E. Segal, and E. Elinav, Microbiota-Modulated Metabolites Shape the Intestinal Microenvironment by Regulating NLRP6 Inflammasome Signaling. Cell 163 (2015) 1428-43.
[44] K. Radulovic, S. Normand, A. Rehman, A. Delanoye-Crespin, J. Chatagnon, M. Delacre, N. Waldschmitt, L.F. Poulin, J. Iovanna, B. Ryffel, P. Rosenstiel, and M. Chamaillard, A dietary flavone confers communicable protection against colitis through NLRP6 signaling independently of inflammasome activation. Mucosal Immunol 11 (2018) 811-819.
[45] N. Segata, J. Izard, L. Waldron, D. Gevers, L. Miropolsky, W.S. Garrett, and C. Huttenhower, Metagenomic biomarker discovery and explanation. Genome Biol 12 (2011) R60.
[46] L. Ghimire, S. Paudel, L. Jin, and S. Jeyaseelan, The NLRP6 inflammasome in health and disease. Mucosal Immunol (2020).
[47] X. Wu, Z. Zeng, H. Tian, L. Peng, D. Xu, Y. Wang, C. Ye, Y. Peng, and R. Fang, The important role of NLRP6 inflammasome in Pasteurella multocida infection. Vet Res 53 (2022) 81.
[48] Q. Tao, D. Xu, K. Jia, X. Cao, C. Ye, S. Xie, D.L. Hu, L. Peng, and R. Fang, NLRP6 Serves as a Negative Regulator of Neutrophil Recruitment and Function During Streptococcus pneumoniae Infection. Front Microbiol 13 (2022) 898559.
[49] R. Boixeda, P. Almagro, J. Diez-Manglano, F.J. Cabrera, J. Recio, I. Martin-Garrido, and J.B. Soriano, Bacterial flora in the sputum and comorbidity in patients with acute exacerbations of COPD. Int J Chron Obstruct Pulmon Dis 10 (2015) 2581-91.
[50] S. Sethi, N. Evans, B.J. Grant, and T.F. Murphy, New strains of bacteria and exacerbations of chronic obstructive pulmonary disease. N Engl J Med 347 (2002) 465-71.
[51] J.A. Wedzicha, and T.A. Seemungal, COPD exacerbations: defining their cause and prevention. Lancet 370 (2007) 786-96.
[52] J. Mei, Y. Liu, N. Dai, M. Favara, T. Greene, S. Jeyaseelan, M. Poncz, J.S. Lee, and G.S. Worthen, CXCL5 regulates chemokine scavenging and pulmonary host defense to bacterial infection. Immunity 33 (2010) 106-17.
[53] T.H. Thatcher, N.A. McHugh, R.W. Egan, R.W. Chapman, J.A. Hey, C.K. Turner, M.R. Redonnet, K.E. Seweryniak, P.J. Sime, and R.P. Phipps, Role of CXCR2 in cigarette smoke-induced lung inflammation. Am J Physiol Lung Cell Mol Physiol 289 (2005) L322-8.
[54] S. Huot-Marchand, M. Nascimento, E. Culerier, M. Bourenane, F. Savigny, C. Panek, C. Serdjebi, M. Le Bert, V.F.J. Quesniaux, B. Ryffel, P. Broz, N. Riteau, A. Gombault, and I. Couillin, Cigarette smoke-induced gasdermin D activation in bronchoalveolar macrophages and bronchial epithelial cells dependently on NLRP3. Front Immunol 13 (2022) 918507.

[55] J.K. Volk, E.E.L. Nystrom, S. van der Post, B.M. Abad, B.O. Schroeder, A. Johansson, F. Svensson, S. Javerfelt, M.E.V. Johansson, G.C. Hansson, and G.M.H. Birchenough, The Nlrp6 inflammasome is not required for baseline colonic inner mucus layer formation or function. J Exp Med 216 (2019) 2602-2618.
[56] J. Yu, T. Liu, Q. Guo, Z. Wang, Y. Chen, and Y. Dong, Disruption of the Intestinal Mucosal Barrier Induced by High Fructose and Restraint Stress Is Regulated by the Intestinal Microbiota and Microbiota Metabolites. Microbiol Spectr 11 (2023) e0469822.
[57] M. Mamantopoulos, F. Ronchi, F. Van Hauwermeiren, S. Vieira-Silva, B. Yilmaz, L. Martens, Y. Saeys, S.K. Drexler, A.S. Yazdi, J. Raes, M. Lamkanfi, K.D. McCoy, and A. Wullaert, Nlrp6- and ASC-Dependent Inflammasomes Do Not Shape the Commensal Gut Microbiota Composition. Immunity 47 (2017) 339-348 e4.
[58] P. Lemire, S.J. Robertson, H. Maughan, I. Tattoli, C.J. Streutker, J.M. Platnich, D.A. Muruve, D.J. Philpott, and S.E. Girardin, The NLR Protein NLRP6 Does Not Impact Gut Microbiota Composition. Cell Rep 21 (2017) 3653-3661.
[59] G.C. Parkes, K. Whelan, and J.O. Lindsay, Smoking in inflammatory bowel disease: impact on disease course and insights into the aetiology of its effect. J Crohns Colitis 8 (2014) 717-25.
[60] J. Cosnes, Smoking and Diet: Impact on Disease Course? Dig Dis 34 (2016) 72-7.
[61] R.P. Young, R.J. Hopkins, and B. Marsland, The Gut-Liver-Lung Axis. Modulation of the Innate Immune Response and Its Possible Role in Chronic Obstructive Pulmonary Disease. Am J Respir Cell Mol Biol 54 (2016) 161-9.
[62] A. Vaughan, Z.A. Frazer, P.M. Hansbro, and I.A. Yang, COPD and the gut-lung axis: the therapeutic potential of fibre. J Thorac Dis 11 (2019) S2173-S2180.
[63] K.L. Bowerman, S.F. Rehman, A. Vaughan, N. Lachner, K.F. Budden, R.Y. Kim, D.L.A. Wood, S.L. Gellatly, S.D. Shukla, L.G. Wood, I.A. Yang, P.A. Wark, P. Hugenholtz, and P.M. Hansbro, Disease-associated gut microbiome and metabolome changes in patients with chronic obstructive pulmonary disease. Nat Commun 11 (2020) 5886.
[64] A.J. Dicker, M.L. Crichton, E.G. Pumphrey, A.J. Cassidy, G. Suarez-Cuartin, O. Sibila, E. Furrie, C.J. Fong, W. Ibrahim, G. Brady, G.G. Einarsson, J.S. Elborn, S. Schembri, S.E. Marshall, C.N.A. Palmer, and J.D. Chalmers, Neutrophil extracellular traps are associated with disease severity and microbiota diversity in patients with chronic obstructive pulmonary disease. J Allergy Clin Immunol 141 (2018) 117-127.
[65] E. Dima, A. Kyriakoudi, M. Kaponi, I. Vasileiadis, P. Stamou, A. Koutsoukou, N.G. Koulouris, and N. Rovina, The lung microbiome dynamics between stability and exacerbation in chronic obstructive pulmonary disease (COPD): Current perspectives. Respir Med 157 (2019) 1-6.
[66] A. Krumina, M. Bogdanova, S. Gintere, and L. Viksna, Gut-Lung Microbiota Interaction in COPD Patients: A Literature Review. Medicina (Kaunas) 58 (2022).
[67] L. Wang, Y. Cai, J. Garssen, P.A.J. Henricks, G. Folkerts, and S. Braber, The Bidirectional Gut-Lung Axis in Chronic Obstructive Pulmonary Disease. Am J Respir Crit Care Med 207 (2023) 1145-1160.
[68] S. Takahashi, M. Ishii, H. Namkoong, A.E. Hegab, T. Asami, K. Yagi, M. Sasaki, M. Haraguchi, M. Sato, N. Kameyama, T. Asakura, S. Suzuki, S. Tasaka, S. Iwata, N. Hasegawa, and T. Betsuyaku, Pneumococcal Infection Aggravates Elastase-Induced Emphysema via Matrix Metalloproteinase 12 Overexpression. J Infect Dis 213 (2016) 1018-30.

[69] X. Tian, J. Hellman, and A. Prakash, Elevated Gut Microbiome-Derived Propionate Levels Are Associated With Reduced Sterile Lung Inflammation and Bacterial Immunity in Mice. Front Microbiol 10 (2019) 159.
[70] H. Hara, S.S. Seregin, D. Yang, K. Fukase, M. Chamaillard, E.S. Alnemri, N. Inohara, G.Y. Chen, and G. Nunez, The NLRP6 Inflammasome Recognizes Lipoteichoic Acid and Regulates Gram-Positive Pathogen Infection. Cell 175 (2018) 1651-1664 e14.
[71] N. Li, X. Yi, C. Chen, Z. Dai, Z. Deng, J. Pu, Y. Zhou, B. Li, Z. Wang, and P. Ran, The gut microbiome as a potential source of non-invasive biomarkers of chronic obstructive pulmonary disease. Front Microbiol 14 (2023) 1173614.